Hydrogenation of Xylose to Xylitol in the Presence of Bimetallic Nanoparticles Ni3Fe Catalyst in the Presence of Choline Chloride

Naseeb Ullah, François Jérôme, Karine de Oliveira Vigier

catalysts

MDPI

Article

Hydrogenation of Xylose to Xylitol in the Presence of Bimetallic Nanoparticles Ni_3Fe Catalyst in the Presence of Choline Chloride

Naseeb Ullah, François Jérôme and Karine De Oliveira Vigier *

Institut de Chimie Des Milieux et Des Matériaux de Poitiers (IC2MP), Université de Poitiers, UMR 7285 CNRS, 1 Rue Marcel Doré, CEDEX 9, 86073 Poitiers, France; naseeb.naseebullah@univ-poitiers.fr (N.U.); francois.jerome@univ-poitiers.fr (F.J.)
* Correspondence: karine.vigier@univ-poitiers.fr

Abstract: Hydrogenation of sugars to sugars alcohols is of prime interest for food applications for instance. Xylose obtained from the hemicellulose fraction of lignocellulosic biomass can be hydrogenated to xylitol. Herein, we conducted catalytic hydrogenation reactions in a non-conventional media approach by using choline chloride, a non-toxic naturally occurring organic compound that can form a deep eutectic solvent with xylose. Acknowledging the benefits of cost-effective transition metal-based alloys, Ni_3Fe_1 bimetallic nanoparticles were utilized as a hetero-catalyst. Under optimized reaction conditions (110 °C, 3 h and 30 bar H_2), a highly concentrated feed of xylose (76 wt.%) was converted to 80% of xylitol, showing the benefit of using choline chloride. Overall, the catalytic conversion activity and the product selectivity in the substrate-assisted DES media are relatively high but, the recyclability of the catalyst should be improved in the presence of such media.

Keywords: hydrogenation; sugars; deep eutectic solvents

Citation: Ullah, N.; Jérôme, F.; De Oliveira Vigier, K. Hydrogenation of Xylose to Xylitol in the Presence of Bimetallic Nanoparticles Ni_3Fe Catalyst in the Presence of Choline Chloride. *Catalysts* **2022**, *12*, 841. https://doi.org/10.3390/catal12080841

Academic Editor: Young-Woong Suh

Received: 29 June 2022
Accepted: 27 July 2022
Published: 30 July 2022

1. Introduction

Due to the depletion of fossil carbon and environmental concerns, high interest is devoted to the use of renewable carbon for fuels and chemicals [1,2]. Lignocellulosic biomass is of particular interest, and carbohydrates represent around 75% of the composition of lignocellulose; indeed, they can be converted to a wide range of molecules with potential functional properties [3,4]. Particularly, the hydrogenation of hemicellulose-derived sugar to produce their corresponding sugar alcohols is attracting significant research interest to establish sustainable platform chemicals. Sugar alcohols find applications in food (sugar-free chewing gums, sugar-free chocolates, sugar-free candies, sugar-free cakes, sugar-free drinks and fruit jellies, sugar-free mints, etc.), beverages (such as freshener, the sweetener in beverages such as in milk, soft drinks, coffee), pharmaceuticals (for diabetes, health drinks, digestive drugs, throat soother, cough syrup), health and personal care (flavouring agent; humectant; skin-conditioning agent, face cream, beauty cream, cleaner, toothpaste, mouth cleansers, etc.) and in animal feed products (poultry feed/animal feed such as in dog food) [5,6]. Furthermore, the sweetening capacity of xylitol exceeds that of saccharose by 20–25% [7]. Xylitol is produced by catalytic hydrogenation of xylose in triphasic batch reactors, in an aqueous medium. Precious metals (i.e., Pt, Pd, Ru, Rh) are active in the hydrogenation of sugars to sugar alcohols and they are stable. More specifically, ruthenium (Ru) and palladium (Pd) exhibit the highest activity and selectivity [8]; however, the use of expensive metal-catalysts limit the economic feasibility of reactions at an industrial scale. Raney Ni catalyst is the most used catalyst in this reaction owing to its activity and lower price compare to noblemetals-based catalysts [9,10]; however, during this reaction, nickel leaches which is detrimental to the applications of sugar alcohols. Hence, a purification of product to remove residual Ni is required, rendering this process economically less

attractive [11]. Therefore, abundant transition metals catalysts (i.e., Cu, Co and Fe) are considered. The addition of a second metal to Ni (i.e., Ni-Fe, Ni-Co and Ni/Cu) can be advantageous due to its low-price value and availability and with the probability to promote the catalytic activity to great extent and can help to increase the stability of the catalyst by synergy effect [12]. Beyond organic conversion reaction, the potential of binary NiFe alloys has been established as highly efficient electrocatalysts for the oxygen evolution reaction. Remarkably, the electrochemical performance originated from the synergistic effects of Fe incorporation into Ni species, leading to the improved charge transfer kinetics and intrinsic activity of the catalyst [13]. Furthermore, dry reforming of methane application, involves the catalytic reforming of methane with carbon dioxide as the oxidant to produce syngas (CO and H_2). Produced syngas can be directly used as fuel or converted into hydrocarbons for specific chemicals' production such as methanol (CH_3OH), and liquid synthetic motor fuels (gasoline, naphtha, kerosene and diesel) [14]; moreover, Ni and Ni-based nanoalloys are also successfully reported for the treatment of industrial wastewater containing toxic dyes [15,16].

In recent years, deep eutectic solvents (DES) are widely studied as environmentally benign alternatives to conventional solvents since DES can be prepared using nontoxic and renewable chemicals [17]. Generally, DES are composed of two compounds, a hydrogen bond donor (HBD) and a hydrogen bond acceptor (HBA) mixed in such a ratio that the resulting substance has a significantly lower melting than the one of each individual component [18]. The most common DES is based on choline chloride (ChCl), carboxylic acids and other HBDs, such as urea, citric acid, succinic acid, and glycerol [19]. In fact, the interaction of the HBD with the quaternary salt reduces the anion–cation electrostatic force, thus decreasing the freezing point of the mixture [20]. DES share many similar features with ionic liquids (ILs), such as low vapour pressure, but are cheaper to produce, both due to the lower cost of the required raw materials and the simplicity of the synthesis [21]. Furthermore, they are less toxic and often biodegradable [22]. Choline chloride (ChCl) can be used as HBA and D-xylose as an HBD source since it can form DES with ChCl; moreover, it was shown previously, that ChCl can help to convert a high concentrated feed of xylose to furfural [23]; this specific behaviour is interesting in order to increase the productivity (kg of product formed per volume per hour) of the process. Hence, this is a key parameter of the process that should be addressed for an industrial application.

In this work, the hydrogenation of a high concentrated feed of xylose to xylitol was studied in the presence of nickel-iron bimetallic nanoparticles (BMNPs) prepared by a one-pot hydrothermal reaction in the presence of ChCl (Scheme 1). The Ni_3Fe_1 BMNPs catalyst was chosen due to the fact that BMNPs displayed higher catalytic efficiencies in contrast to their monometallic counterparts, due to their strong synergy between the metals and this ratio proving to be the efficient one for such reaction [24]. Particularly, Ni-based bimetallic catalyst exhibit specific properties, via a synergistic or bi-functional effect, which differs from those of the parent metals and offers the opportunity to design catalysts with bimetallic particles composition; this can affect their catalytic properties and these parameters should be precisely characterized and optimized in order to correlate the catalyst formulation and its performances in reaction [25]. The effect of various reaction parameters is discussed in detail as well as the stability of the catalyst in this reaction media.

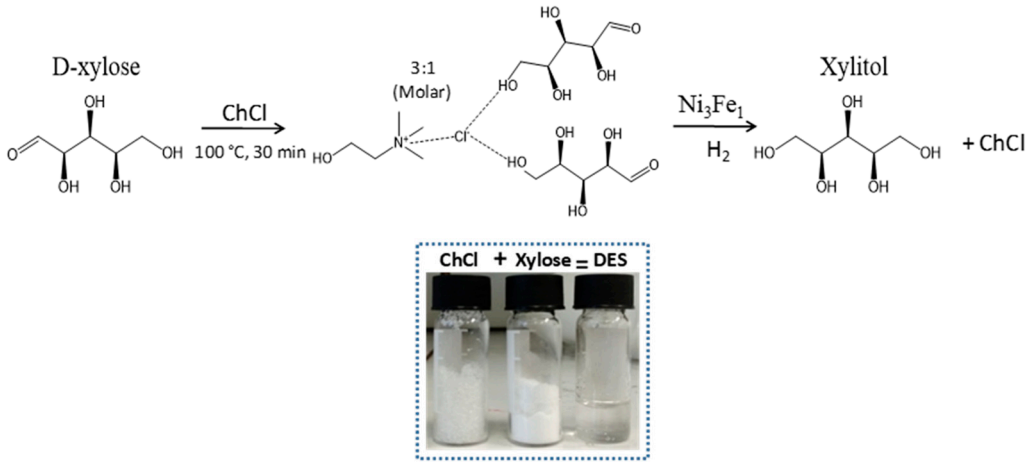

Scheme 1. DES phase hydrogenation of D-xylose into Xylitol.

2. Results/Discussion

2.1. Effect of Reaction Media

A DES solvent with a composition of 1:2 (D-xylose:ChCl) molar ratio was prepared by keeping the mixture for 30–40 min intervals at constant stirring and heating up to 100 °C temperature, which is obviously lower than the actual melting point of both individual DES components (ChCl = 302 °C, D-xylose = 145 °C). Notably, the as-prepared DES exhibits a neutral pH in the mixture, which may be very useful for envisaging DES applications. No purification step is needed, contributing to their promise as economically viable alternatives to conventional organic solvents and ionic liquids [21]. In order to set out optimized parameters for the DES-phase hydrogenation reaction, several experiments were conducted. Primarily, in the pure DES (1.5 g, containing 33 wt% of xylose) reaction media with a composition of 1:2 (D-xylose/ChCl) molar ratio and Ni_3Fe_1 BMNPs as catalyst under mild conditions (cat. 70 mg, H_2 = 30 bar, T = 110 °C, 3 h) were tested. As shown in Figure 1, an intermediate yield of xylitol (38%) was achieved for 57% xylose conversion. One can mention that ChCl and xylitol can form also a DES. A blank reaction was performed using bare choline chloride under a hydrogenation atmosphere and no product was detected suggesting that the hydrogenation does not affect the choline chloride.

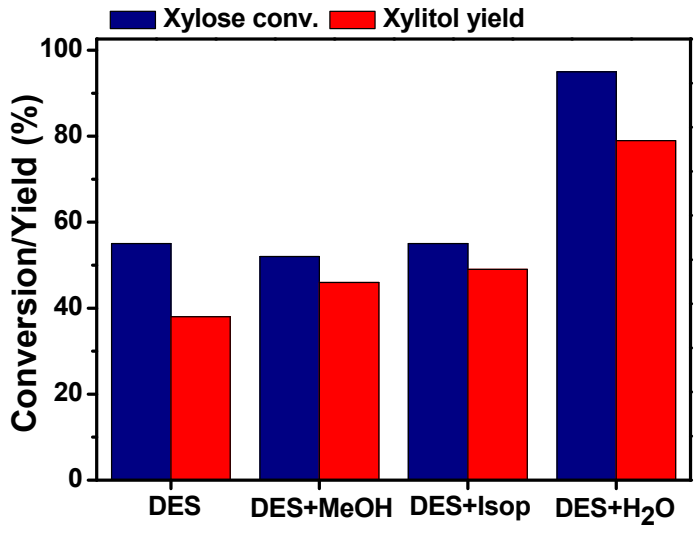

Figure 1. Effect of different solvents in DES phase reaction (reaction conditions: cat. 70 mg, 1.5 g of $DES_{(1:2)}$, 0.5 mL of solvent, H_2 = 30 bar, T = 110 °C, 3 h).

This can be ascribed to the high viscosity of pure DES. Hence, it is known that one drawback of DESs in a chemical reaction can be their high viscosity. Generally, few amounts of solvents are added to DESs in order to decrease the viscosity. Consequently, an appropriate amount of water, methanol (MeOH) and isopropanol (up to 33 wt.%) was introduced to the DES (1:2). No increase in the xylose conversion in the xylitol yield was observed when methanol or isopropanol were added, whereas an increase up to 79% yield of xylitol was achieved by using water DES combination. By-products are formed that were difficult to analyze; they can be condensation, and degradation compounds obtained from the sugar. These results suggest that it was not only a question of viscosity, since it was decreased when methanol, isopropanol and water was added; however, a synergistic effect of DES and H_2O was observed in the reaction system. Many theoretical and experimental experiments were performed in order to understand the effect of water on the nanostructure of DESs and are reported in the literature [26]. The addition of water can change their structure since the H-bonding network will be weakened by the addition of water until it becomes a solution of DES components in water [27,28]. The amount of water that can be added is directly correlated to the nature of the eutectic mixture composition. The effect of water addition on the nanostructure of several choline chloride-based DESs was investigated in the literature with different technics (neutron total scattering and empirical potential structure refinement (EPSR) [24], ^{1}H NMR [25] FTIR and Raman spectroscopy [29]; these studies show that the supramolecular structure of the DESs is preserved up to 40 ÷ 50%water (0.8 ÷ 0.9 molar fraction). Above this water loading, the DES components are completely dissociated and hydrated and the system becomes an aqueous solution of HBA and HBD; this was confirmed by molecular dynamics simulations showing that when water is added in small amounts, it gets adsorbed in the structure of the DESs and the hydrogen bond interactions of the liquid do not change [30–32]. In this study, a slight addition of water favoured the hydrogenation reaction without affecting the DES composition, probably due to an increase in the hydrogen dissolution.

2.2. Effect of Molar Ratio D-Xylose/ChCl

Keeping in mind that the challenge was to use a highly concentrated feed of xylose, Ni_3Fe_1 BMNPs were used in a series of DES with the variable composition of ChCl and D-xylose. The amount of added water was always the same as well as the amount of catalyst used (70 mg). As presented in Figure 2, the yield of sugar alcohol decreases with the increase in the initial molar ratio D-Xylose: ChCl; this can be due to the insufficient amount of catalyst related to xylose content in the reaction system. With the amount of this catalyst, $DES_{(1:2)}$ was found more efficient during hydrogenation reaction due to an appropriate amount; however, the increase in xylose concentration is highly demanded to obtain high productivity of the process, and thus, the $DES_{(3:1)}$ composition was further studied, since it could allow converting a high concentrated feed of xylose (76 wt.% in the DES).

In order to increase the yield, the effect of catalysts amount was studied using different amounts of Ni_3Fe_1 BMNPs catalyst while keeping other operation parameters constant (Figure 3). A progressive trend can be observed in the production of sugar alcohols and substrate conversion until the optimized point is reached when 100 mg (8.9 wt%) catalyst was used. Nonetheless, the excess of catalyst beyond the optimized point (over 8.9 wt.%) causes a decline in the product yield, most probably due to degradation reactions that are also favoured with the increase of the catalyst loading; this result shows the efficiency of the catalyst in a DES phase containing a high concentration of xylose (76 wt% in the DES and 57 wt% in the DES/H_2O media). In the literature, with a xylose loading of 50 wt%, the yield was below 50%, showing the benefit of using a mixture ChCl/H_2O for the hydrogenation of a high concentrated feed of xylose which is of prime importance to increase the productivity of the process. Hence, in this experiment, the productivity was around 5 kg/m^3/h.

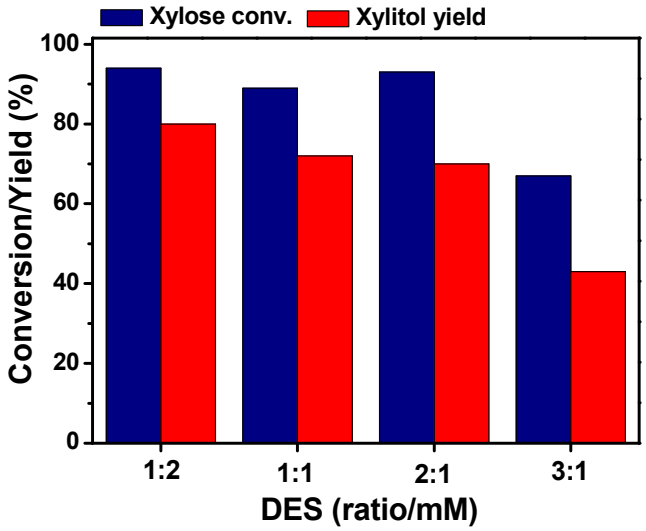

Figure 2. Effect of composition of DES components (reaction conditions: 1.5 g of DES, 0.5 mL of H_2O, cat. 70 mg, H_2 = 30 bar, T = 110 °C, 3 h).

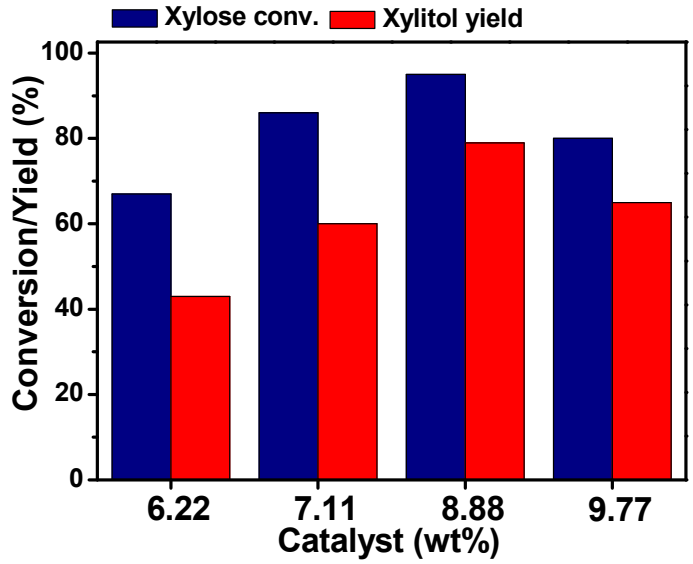

Figure 3. Effect of catalyst concentration/mass (reaction conditions: 1.5 g of $DES_{(3:1)}$, H_2 = 30 bar, T = 110 °C, 3 h).

2.3. Effect of the Reaction Temperature

The effect of the temperature was then studied (Figure 4). When the temperature was increased from 110 °C to 120 °C, the conversion was similar but the yield in xylitol dropped from 79% to 51%; this was due to the formation of undetermined by-products such as humins. Hence, the solution was dark brown showing the formation of degradation products. A decrease in the temperature from 110 °C down to 80 °C led to a decrease in the xylose conversion from 79% to 65% along with a decrease in the yield in xylitol from 79% to 46%. The selectivity of the reaction was in the range of 70% to 80% for temperature range from 80 °C to 110 °C. At 80 °C, the reaction was prolonged up to 6 h, and we were pleased to see that 94% of xylose was converted to 70% of xylitol (75% of selectivity in xylitol). Hence, it is a compromise between the temperature and the reaction time; however, the maximum temperature should be 110 °C in order to avoid side reactions.

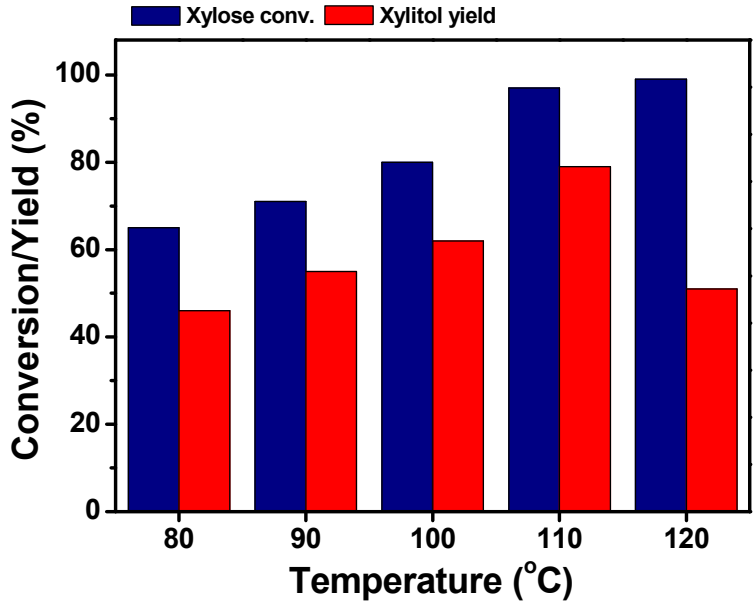

Figure 4. Effect of different temperature on DES phase reaction (reaction conditions: cat. 70 mg, 1.5 g of $DES_{(3:1)}$, 0.5 mL of solvent, H_2 = 30 bar, 3 h).

2.4. Stability of the Ni_3Fe_1 BMNPs

One important parameter is the stability of the Ni_3Fe_1 BMNPs; thus, this was examined by consecutively repeating the DES phase hydrogenation reaction under optimized conditions (H_2 = 30 bar, 3 h, 110 °C). To this end, the catalyst was magnetically recovered and washed thoroughly with distilled water and methanol (3 × 10 mL) in an ultrasonic bath sonicator at room temperature (25 °C). Then, the used catalyst was reused with a fresh charge of sugar for subsequent recycle runs under the same reaction conditions. Notably, the recovered catalyst was processed consecutively for the next run without involving reactivation steps. As shown in Figure 5, after each run the xylose conversion decreased from 91% to 54% and subsequently to 41%. A similar trend can be consecutively noticed in the xylitol yield from 79% down to 35% and then down to 27% for the third cycle.

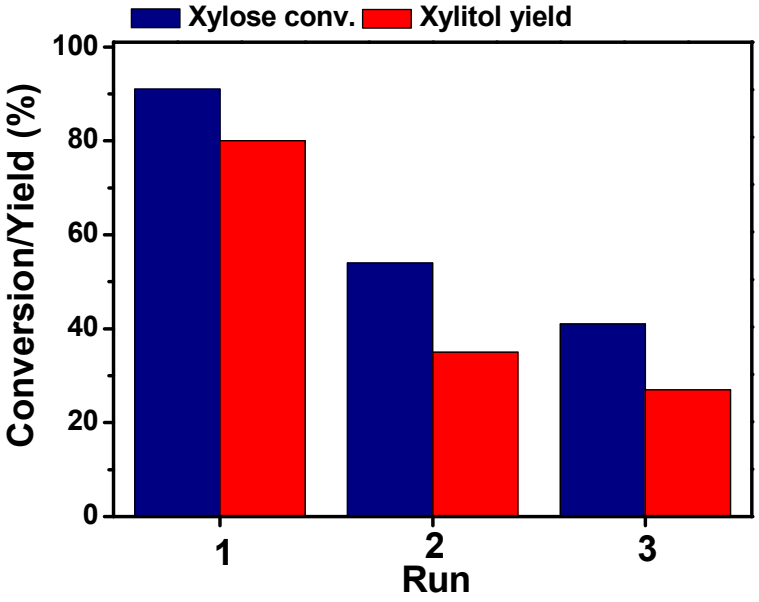

Figure 5. Recyclability potential of Ni_3Fe_1 BMNPs in DES-phase catalytic hydrogenation of sugar (cat. 100 mg, $DES_{(3:1)}$, H_2 = 30 bar, T = 110 °C, 3 h).

In order to investigate the faster deactivation of the Ni_3Fe_1 BMNPs in DES phase reaction, the spent catalyst was analyzed under microscopic (TEM) analysis. Upon comparative study of microscopic analysis with fresh catalyst, it was demonstrated that the deactivation of Ni_3Fe_1 BMNPs in the DES phase is mainly occurring by the strong adsorption of organic species in metallic phase, and thus blocking the active sites for the hydrogenation of xylose (Figures 6 and 7) [32,33]. Furthermore, EDS analysis of individual Ni_3Fe_1 BMNPs was also performed to examine the effect of the leaching behaviour of Ni and Fe metals (as shown in Figure 8). The results show that the particles are stable and no severe loss of metal is detected that can possibly cause changes in the synergic efficacy of the bimetallic nanoparticles. Hence, it reveals that the deactivation of the catalyst can occur due to the strong chemisorption of organic species on catalytic sites, thereby blocking sites for the catalytic reaction [34,35].

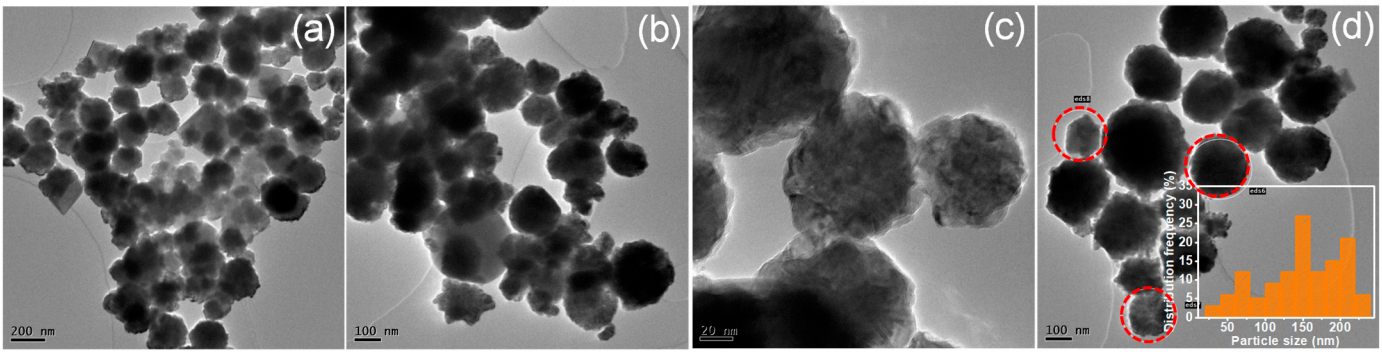

Figure 6. (**a**–**d**) Microscopic analysis (TEM) of fresh Ni_3Fe_1 BMNPs at different magnification and inset (**d**) particle size distribution histogram of Ni_3Fe_1 BMNPs.

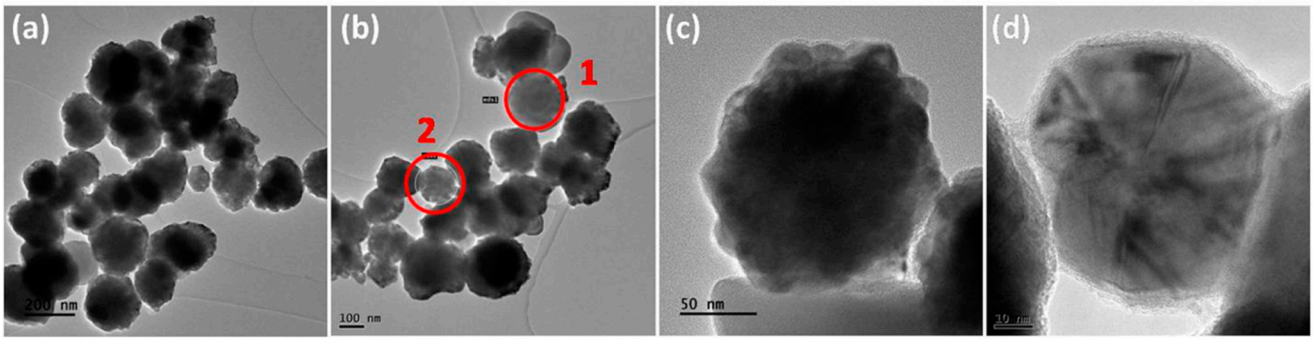

Figure 7. (**a**–**d**). Microscopic analysis (TEM) of the recycled Ni_3Fe_1 BMNPs at different magnification was obtained after the DES-phase hydrogenation reaction.

Additionally, to gain more knowledge about the deactivation of catalyst in the DES phase hydrogenation reaction, thermogravimetric analysis (TGA) of both fresh and spent catalyst was performed (Figure 9). The isolated spent catalyst was washed with H_2O and with other organic solvents (acetone/ethanol). The obtained results show that using only H_2O solvent is not sufficient to remove the surface adsorbed organic species. Despite the fact that the TGA analysis of the spent catalyst washed with a mixture of acetone/ethanol showed a similar profile to the fresh one, the catalyst was not as active as in the first cycle. It suggests that strong adsorption of organic compounds occurs in the hydrogenation of xylose in DES-phase reaction; moreover, in the liquid phase 70 ppm of Fe was analyzed by ICP-OES analysis and the amount of Ni leached was 9 ppm, 27 ppm and 17 ppm, respectively, after the first, second and third cycle (Table 1) showing that he catalyst was not stable in this reaction media. If thermal treatment is used, non-supported Ni_3Fe_1 BMNPs are more likely to aggregate and this may affect the catalytic activity; that is the reason why the preparation method is under investigation in our group.

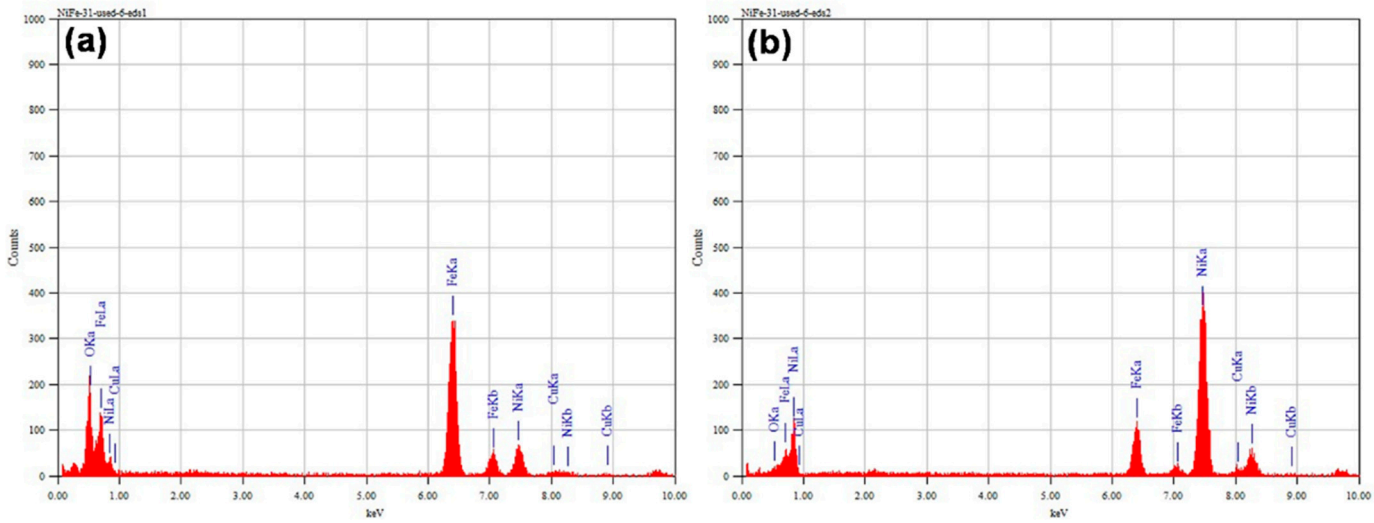

Figure 8. (**a**,**b**). EDS spectrum of recycled individual Ni_3Fe_1 BMNPs obtained after DES-phase hydrogenation reaction.

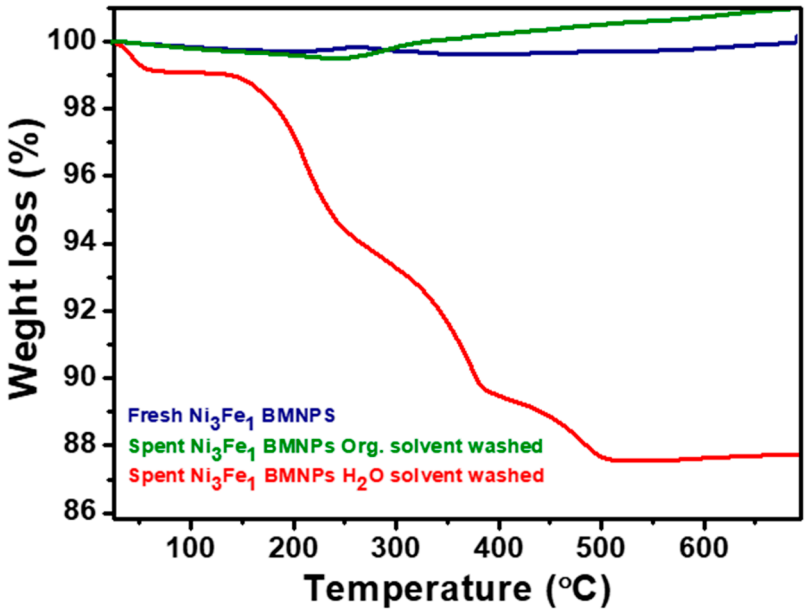

Figure 9. Thermogravimetric analysis (TGA) of fresh and spent Ni_3Fe_1 BMNPs after washing for recycling experiments.

Table 1. ICP-OES analysis of catalytic product in DES-phase hydrogenation reaction by Ni_3Fe_1 BMNPs.

Ni_3Fe_1 BMNPs	Fe (238, 204 nm) mg/L	Ni (216, 555 nm) mg/L
1	69.9	8.7
2	74.8	27.0
3	71.3	17.4

3. Materials and Methods

3.1. Chemicals

Ferrous sulfate ($FeSO_4 \cdot 7H_2O$), nickel (II) chloride ($NiCl_2$), sodium hydroxide (NaOH), hydrazine hydrate ($H_2NNH_2 \cdot H_2O$) and ethylene glycol ($HOCH_2CH_2OH$) was obtained from Merck. The Choline chloride ($(CH_3)_3N(Cl)CH_2CH_2OH$) with ≥98% purity, and sugar substrates such as D-xylose were acquired commercially and used as received.

3.2. Synthesis of Ni_3Fe_1 Bimetallic Nanoparticles (BMNPs)

The Ni_3Fe_1 bimetallic nanoparticles (BMNPs) were synthesized by using the hydrothermal method. Typically, $FeSO_4{\cdot}7H_2O$ and $NiCl_2$ in a certain molar ratio (3:1) of Ni:Fe were dissolved into 200 mL of deionized water and ethylene glycol solution. One can mention that using iron chloride salt no reduction in hydrothermal treatment was observed. That is the reason why, according to the literature, iron sulfate was chosen. Afterwards, NaOH (16 mL, 1 M) solution was added to the mixture dropwise and the pH value was adjusted to around 9 and hydrazine hydrate (2 mL) was used as a reducing agent. The mixture solution was well stirred under an N_2 atmosphere and then transferred to a Teflon-lined stainless steel autoclave. The autoclave was sealed and placed in a heating furnace adjusted at 125 °C for 16 h. After the reaction, the reactor was cooled down to room temperature naturally and the as-prepared Ni_3Fe_1 BMNPs (black solid phase) were separated by using a magnetic bar. Finally, the obtained product was washed and re-dispersed in deionized water and methanol several times and vacuum dried. The Ni and Fe content was determined by ICP-OES analysis and was 22 wt.% and 72 wt.%, respectively.

3.3. Catalyst Characterizations

Powder X-ray diffraction (XRD) was performed using a Bruker D8 Advance diffractometer with Cu Kα radiation. The operating voltage and current were 40 kV and 40 mA, respectively. The step length was 0.02° with a scanning rate of 2°/min from 10–95° (Figure S1).TEM analysis was performed using a JEOL JEM 2100 UHR equipped with a LaB6 filament with a punctual resolution of 0.19 nm. The samples were prepared in ethanol using a sonication bath and some drops were deposited on a carbon grid (Holey Carbon grids). Thermal analysis was performed using a TA instrument, SDTQ 600 under air with a flow rate of 100 mL/min with a ramp of 10 °C/min. A PerkinElmer SCIEX ICP Mass Spectrometer Elan 6100 DRC Plus and an Optima 5300DV ICP Optical Emission Spectrometer were used to measure the Ni-Fe contents in the reaction medium. The nanoparticles were digested in 5% nitric acid in a 1:20 dilution from a 1 g/L nanoparticle suspension. The detection limits were 0.014 ppm for Fe and 0.018 ppm for Ni.

3.4. Hydrogenation of Xylose to Xylitol

In the preparation of DES for the reaction, ChCl was first vacuum dried for 24 h at 60 °C. Then, xylose was precisely added and the mixture was heated and stirred until a clear and homogeneous liquid was formed. One can mention that for D-Xylose: ChCl DES, without water the optimum ratio was 1:1 to reach a minimum melting point [36]; however, water was added to our system and as reported in the literature for a D-xylose:ChCl with a molar ratio of 1:2, the melting point was 78.3 °C with 3.8 wt% of water [37]. For the D-Xylose:ChCl molar ratio of 1:2 the melting enthalpy was 2.947 kJ/mol. When using the as-prepared DES in hydrogenation reaction, a known mass of the Ni_3Fe_1 BMNPs was added and super-sonicated to ensure the maximum dispersion. Finally, the prepared DES-catalyst mixture was shifted to a mechanically driven stainless steel autoclave reactor (25 mL, PARR 5500, Moline, IL, USA), sealed and flushed with N_2 and then pressurized with H_2 gas up to desired pressure at ambient temperature. Upon completion of reaction time, the reactor was allowed to cool down to room temperature (RT) naturally and the unreacted H_2 gas was vented off. The resultant catalytic mixture product was diluted with deionized water to a certain volume and then the catalyst was eliminated by using a permanent magnet bar. The product was quantitatively analyzed by HPLC-RID (LC-20AD Shimadzu-Japan) equipped with an auto sampler assembly SIL-10A and a controller CBM 20A. The products were separated on Varian 100-5 amino S 250 × 4.6 mm (NH_2) column using acetonitrile/water (80/20, vol. ratio) as eluent, the flow rate was kept 0.8 mL.min^{-1} at 40 °C. The refractive index detector (model no. RID-20A) was used for the detection and calibration of compounds.

4. Conclusions

Noble metal-free Ni_3Fe_1 BMNPs have been synthesized hydrothermally and characterized by XRD and TEM analysis. A high concentration of xylose containing DES was prepared as reaction media to assess the catalytic potential of bimetallic nanocatalysts for hydrogenation. The obtained experimental result reveals the catalytic potential of binary metals for the active and selective hydrogenation of a concentrated feed of xylose to xylitol with a high yield (up to 80%) starting from a highly concentrated feed of xylose allowing a productivity of around 5 $kg/m^3/h$. Microscopic and thermal investigation of the recycled Ni_3Fe_1 BMNPs displays the surface adsorbed organic species (likely choline chloride, a DES component) that is blocking the active sites and thus directly affecting the activity in recycling test. Furthermore, the preparation method of such catalyst is under investigation in our group in order to increase the stability of this promising catalyst for the conversion of a high concentrated feed of xylose to xylitol using ChCl.

Supplementary Materials: The following supporting information can be downloaded at: https://www.mdpi.com/article/10.3390/catal12080841/s1, Figure S1: X-ray diffraction (XRD) pattern of as-synthesized Ni_3Fe_1 BMNPs.

Author Contributions: Investigation, N.U., F.J. and K.D.O.V.; Experiment, N.U.; writing—original draft preparation, N.U.; writing—review and editing, F.J. and K.D.O.V.; supervision, K.D.O.V. All authors have read and agreed to the published version of the manuscript.

Funding: This research was funded by ANR for the project NobleFreeCat (ANR-17-CE07-0022) and thus the grant for the post-doctoral position of Naseeb Ullah.

Acknowledgments: The authors acknowledge ANR for the funding of the project NobleFreeCat (ANR-17-CE07-0022) and thus the grant for the post-doctoral position of Naseeb Ullah; they are grateful to the region Nouvelle Aquitaine for the CPER and EU-FEDER support, to INCREASE Federation and to the GDR 2035 SolvATE; this work pertains to the French government program "Investissements d'Avenir" (EUR INTREE, reference ANR-18-EURE-0010).

Conflicts of Interest: The authors declare no conflict of interest.

References

1. Questell-Santiago, Y.M.; Galkin, M.V.; Barta, K.; Luterbacher, J.S. Stabilization strategies in biomass depolymerization using chemical functionalization. *Nat. Rev. Chem.* **2020**, *4*, 311–330. [CrossRef]
2. Stuhr, R.; Bayer, P.; Stark, C.B.W.; von Wangelin, A.J. Light-Driven Waste-To-Value Upcycling: Bio-Based Polyols and Polyurethanes from the Photo-Oxygenation of Cardanols. *ChemSusChem* **2021**, *14*, 3325–3332. [CrossRef] [PubMed]
3. Kazachenko, A.; Akman, F.; Medimagh, M.; Issaoui, N.; Vasilieva, N.; Malyar, Y.N.; Sudakova, I.G.; Karacharov, A.; Miroshnikova, A.; Al-Dossary, O.M. Sulfation of Diethylaminoethyl-Cellulose: QTAIM Topological Analysis and Experimental and DFT Studies of the Properties. *ACS Omega* **2021**, *6*, 22603–22615. [CrossRef]
4. Fineberg, S.J.; Nandyala, S.V.; Marquez-Lara, A.; Oglesby, M.; Patel, A.A.; Singh, K. Incidence and risk factors for postoperative delirium after lumbar spine surgery (Phila Pa 1976). *Spine* **2013**, *38*, 1790–1796. [CrossRef] [PubMed]
5. Lari, G.M.; Gröninger, O.G.; Li, Q.; Mondelli, C.; López, N.; Pérez-Ramírez, J. Catalyst and Process Design for the Continuous Manufacture of Rare Sugar Alcohols by Epimerization-Hydrogenation of Aldoses. *ChemSusChem* **2016**, *9*, 3407–3418. [CrossRef] [PubMed]
6. Yamaguchi, A.; Sato, O.; Mimura, N.; Shirai, M. Catalytic production of sugar alcohols from lignocellulosic biomass. *Catal. Today* **2016**, *265*, 199–202. [CrossRef]
7. Audemar, M.; Ramdani, W.; Junhui, T.; Ifrim, A.R.; Ungureanu, A.; Jérôme, F.; Royer, S.; De Oliveira Vigier, K. Selective Hydrogenation of Xylose to Xylitol over Co/SiO 2 Catalysts. *ChemCatChem* **2020**, *12*, 1973–1978. [CrossRef]
8. Sun, J.; Liu, H. Selective hydrogenolysis of biomass-derived xylitol to ethylene glycol and propylene glycol on supported Ru catalysts. *Green Chem.* **2011**, *13*, 135–142. [CrossRef]
9. Hilpmann, G.; Steudler, S.; Ayubi, M.M.; Pospiech, A.; Walther, T.; Bley, T.; Lange, R. Combining Chemical and Biological Catalysis for the Conversion of Hemicelluloses: Hydrolytic Hydrogenation of Xylan to Xylitol. *Catal. Lett.* **2019**, *149*, 69–76. [CrossRef]
10. Mikkola, J.-P.; Vainio, H.; Salmi, T.; Sjöholm, R.; Ollonqvist, T.; Väyrynen, J. Deactivation kinetics of Mo-supported Raney Ni catalyst in the hydrogenation of xylose to xylitol. *Appl. Catal. A Gen.* **2000**, *196*, 143–155. [CrossRef]
11. Lee, G.D.; Suh, C.S.; Park, J.H.; Park, S.S.; Hong, S.S. Raney Ni catalysts derived from different alloy precursors (I) morphology and characterization. *Korean J. Chem. Eng.* **2005**, *22*, 375–381. [CrossRef]

12. Shi, D.; Wojcieszak, R.; Paul, S.; Marceau, E. Ni Promotion by Fe: What Benefits for Catalytic Hydrogenation? *Catalysts* **2019**, *9*, 451. [CrossRef]
13. Lim, D.; Oh, E.; Lim, C.; Shim, S.E.; Baeck, S.-H. Bimetallic NiFe alloys as highly efficient electrocatalysts for the oxygen evolution reaction. *Catal. Today* **2020**, *352*, 27–33. [CrossRef]
14. Bian, Z.; Das, S.; Wai, M.H.; Hongmanorom, P.; Kawi, S. A Review on Bimetallic Nickel-Based Catalysts for CO_2 Reforming of Methane. *ChemPhysChem* **2017**, *18*, 3117–3134. [CrossRef] [PubMed]
15. Khan, I.; Saeed, K.; Zekker, I.; Zhang, B.; Hendi, A.H.; Ahmad, A.; Ahmad, S.; Zada, N.; Ahmad, H.; Shah, L.A.; et al. Review on Methylene Blue: Its Properties, Uses, Toxicity and Photodegradation. *Water* **2022**, *14*, 242. [CrossRef]
16. Khan, I.; Saeed, K.; Ali, N.; Khan, I.; Zhang, B.; Sadiq, M. Heterogeneous photodegradation of industrial dyes: An insight to different mechanisms and rate affecting parameters. *J. Environ. Chem. Eng.* **2020**, *8*, 104364. [CrossRef]
17. Liu, Y.; Deak, N.; Wang, Z.; Yu, H.; Hameleers, L.; Jurak, E.; Deuss, P.J.; Barta, K. Tunable and functional deep eutectic solvents for lignocellulose valorization. *Nat. Commun.* **2021**, *12*, 1–15. [CrossRef]
18. Zhang, Q.; De Oliveira Vigier, K.; Royer, S.; Jérôme, F. Deep eutectic solvents: Syntheses, properties and applications. *Chem. Soc. Rev.* **2012**, *41*, 7108–7146. [CrossRef] [PubMed]
19. Larriba, M.; Ayuso, M.; Navarro, P.; Delgado-Mellado, N.; Gonzalez-Miquel, M.; García, J.; Rodríguez, F. Choline Chloride-Based Deep Eutectic Solvents in the Dearomatization of Gasolines. *ACS Sustain. Chem. Eng.* **2017**, *6*, 1039–1047. [CrossRef]
20. Hansen, B.B.; Spittle, S.; Chen, B.; Poe, D.; Zhang, Y.; Klein, J.M.; Horton, A.; Adhikari, L.; Zelovich, T.; Doherty, B.W.; et al. Deep Eutectic Solvents: A Review of Fundamentals and Applications. *Chem. Rev.* **2020**, *121*, 1232–1285. [CrossRef] [PubMed]
21. Florindo, C.; Branco, L.C.; Marrucho, I.M. Quest for Green-Solvent Design: From Hydrophilic to Hydrophobic (Deep) Eutectic Solvents. *ChemSusChem* **2019**, *12*, 1549–1559. [CrossRef] [PubMed]
22. Smith, E.L.; Abbott, A.P.; Ryder, K.S. Deep Eutectic Solvents (DESs) and Their Applications. *Chem. Rev.* **2014**, *114*, 11060–11082. [CrossRef]
23. Jiang, S.; Verrier, C.; Ahmar, M.; Lai, J.; Ma, C.; Muller, E.; Queneau, Y.; Pera-Titus, M.; Jérôme, F.; Vigier, K.D.O. Unveiling the role of choline chloride in furfural synthesis from highly concentrated feeds of xylose. *Green Chem.* **2018**, *20*, 5104–5110. [CrossRef]
24. Sadier, A.; Shi, D.; Mamede, A.-S.; Paul, S.; Marceau, E.; Wojcieszak, R. Selective aqueous phase hydrogenation of xylose to xylitol over SiO2-supported Ni and Ni-Fe catalysts: Benefits of promotion by Fe. *Appl. Catal. B Environ.* **2021**, *298*, 120564. [CrossRef]
25. Liu, L.; Gao, F.; Concepción, P.; Corma, A. A new strategy to transform mono and bimetallic non-noble metal nanoparticles into highly active and chemoselective hydrogenation catalysts. *J. Catal.* **2017**, *350*, 218–225. [CrossRef]
26. Ma, C.; Laaksonen, A.; Liu, C.; Lu, X.; Ji, X. The peculiar effect of water on ionic liquids and deep eutectic solvents. *Chem. Soc. Rev.* **2018**, *47*, 8685–8720. [CrossRef] [PubMed]
27. Monroe, D.C.; Blumenfeld, R.S.; Keator, D.B.; Solodkin, A.; Small, S.L. One season of head-to-ball impact exposure alters functional connectivity in a central autonomic network. *NeuroImage* **2020**, *223*, 117306. [CrossRef]
28. Hammond, O.S.; Bowron, D.T.; Edler, K.J. The effect of water upon deep eutectic solvent nanostructure: An unusual transition from ionic mixture to aqueous solution. *Angew. Chem. Int. Ed.* **2017**, *56*, 9782–9785. [CrossRef]
29. Dai, Y.; Witkamp, G.-J.; Verpoorte, R.; Choi, Y.H. Tailoring properties of natural deep eutectic solvents with water to facilitate their applications. *Food Chem.* **2015**, *187*, 14–19. [CrossRef] [PubMed]
30. Ahmadi, R.; Hemmateenejad, B.; Safavi, A.; Shojaeifard, Z.; Shahsavar, A.; Mohajeri, A.; Dokoohaki, M.H.; Zolghadr, A.R. Deep eutectic–water binary solvent associations investigated by vibrational spectroscopy and chemometrics. *Phys. Chem. Chem. Phys.* **2018**, *20*, 18463–18473. [CrossRef]
31. Zhekenov, T.; Toksanbayev, N.; Kazakbayeva, Z.; Shah, D.; Mjalli, F.S. Formation of type III Deep Eutectic Solvents and effect of water on their intermolecular interactions. *Fluid Phase Equilib.* **2017**, *441*, 43–48. [CrossRef]
32. Gao, Q.; Zhu, Y.; Ji, X.; Zhu, W.; Lu, L.; Lu, X. Effect of water concentration on the microstructures of choline chloride/urea (1:2) /water mixture. *Fluid Phase Equilib.* **2018**, *470*, 134–139. [CrossRef]
33. Mikkola, J.-P.; Salmi, T.; Sjöholm, R.; Mäki-Arvela, P.; Vainio, H. Hydrogenation of xylose to xylitol: Three-phase catalysis by promoted raney nickel, catalyst deactivation and in-situ sonochemical catalyst rejuvenation. In *Studies in Surface Science and Catalysis*; Elsevier: Granada, Spain, 2000; Volume 130, pp. 2027–2032. [CrossRef]
34. Besson, M.; Gallezot, P. Deactivation of metal catalysts in liquid phase organic reactions. *Catal. Today* **2003**, *81*, 547–559. [CrossRef]
35. Bartholomew, C.H. Mechanisms of catalyst deactivation. *Appl. Catal. A Gen.* **2001**, *212*, 17–60. [CrossRef]
36. Silva, L.P.; Fernandez, L.; Conceição, J.; Martins, M.A.R.; Sosa, A.; Ortega, J.; Pinho, S.P.; Coutinho, J.A.P. Design and Characterization of Sugar-Based Deep Eutectic Solvents Using Conductor-like Screening Model for Real Solvents. *ACS Sustain. Chem. Eng.* **2018**, *6*, 10724–10734. [CrossRef]
37. Craveiro, R.; Aroso, I.; Flammia, V.; Carvalho, T.; Viciosa, M.T.; Dionísio, M.; Barreiros, S.; Reis, R.L.; Duarte, A.R.C.; Paiva, A. Properties and thermal behavior of natural deep eutectic solvents. *J. Mol. Liq.* **2016**, *215*, 534–540. [CrossRef]